19930104 09

N93-19593

Session II. Hazard Characterization

Three-Dimensional Numerical Simulation of the 20 June 1991, Orlando Microburst

Dr. Fred Proctor, NASA Langley Research Center

PRECEDING PAGE BLANK NOT FILMED

THREE-DIMENSIONAL NUMERICAL SIMULATION OF THE 20 JUNE 1991, ORLANDO MICROBURST

FRED H. PROCTOR

NASA-LANGLEY RESEARCH CENTER
Flight Management Division
HAMPTON, VA 23665

14 APRIL 1992

FOURTH COMBINED MANUFACTURERS' AND TECHNOLOGISTS' WIND SHEAR REVIEW MEETING

OUTLINE OF
ORLANDO 20 JUNE 1991 SIMULATION

I. INTRODUCTION

- A. TASS MODEL DESCRIPTION
- B. INITIAL CONDITIONS

II. RESULTS OF 3-D CASE STUDY

- A. DESCRIPTION OF MICROBURST EVOLUTION
- B. COMPARISON WITH OBSERVATIONS
- C. EVOLUTION OF F-FACTOR FIELDS
- D. COMPARISON OF TEMPERATURE VS F-FACTOR FIELDS

III. SUMMARY

EXTENDED ABSTRACT

On June 20, 1991, NASA's Boeing 737, equipped with in-situ and look-ahead wind-shear detection systems, made direct low-level penetrations (300-350 m AGL) through a microburst during several stages of its evolution. This microburst was located roughly 20 km northeast of Orlando International Airport and was monitored by a Terminal Doppler Weather Radar (TDWR) located about 10 km south of the airport. The first NASA encounter with this microburst (Event #142), at ~2041 UTC, was during its intensification phase. At flight level, in-situ measurements indicated a peak 1-km (averaged) F-factor of ~0.1. The second NASA encounter (Event #143) occurred at ~2046 UTC, about the time of microburst peak intensity. It was during this penetration that a peak 1-km F-factor of ~.17 was encountered, which was the largest in-situ measurement of the 1991 summer deployment. By the third encounter (Event #144), at ~2051 UTC, the microburst had expanded into a macroburst. During this phase of evolution, an in-situ 1-km F-factor of 0.08 was measured. Details of these encounters from the perspective of on-board radar, in-situ observation, on-board infrared sensor and TDWR are discussed by various authors elsewhere in the conference proceedings. The focus of this paper is to examine this microburst *via* numerical simulation from an unsteady, three-dimensional meteorological cloud model. The simulated high-resolution data fields of wind, temperature, radar reflectivity factor, and precipitation are closely examined so as to derive information not readily available from "observations" and to enhance our understanding of the actual event. Characteristics of the simulated microburst evolution are compared with TDWR and in-situ measurements.

The model used in the simulation is the Terminal Area Simulation[1] (TASS), which has been previously applied to a number of microburst case studies.[2,3,4,5,6,7,8] Characteristics of the model are listed in Slide 1 and Tables 1 and 2. The initial conditions for this simulation are listed in Slide 2, and the input sounding for ambient temperature, humidity, and wind is shown in Slide 3. The ambient sounding, observed near the location and time of the microburst, indicates a moist, convectively unstable environment with weak and variable winds.

Results from the simulation are shown in the remaining figures and are summarized in the final slide. The results indicate a high-reflectivity (wet) microburst of moderate intensity whose evolution and structure compare favorably with observations. This microburst, which is generated from the simulated parent

storm, may be characterized by three phases of evolution: 1) an intensification phase, 2) a peak-intensity phase, and 3) a macroburst phase. The intensification phase is initiated by rain forming through collection-coalescence and is associated with increasing values of hazard and velocity differential. According to the model simulation, and verified from "observations", the strongest region of wind-shear hazard at this time is in the northern region of the outflow. The first NASA encounter of the actual microburst took place during this phase of evolution. Several minutes later during the peak-intensity phase, a second surge of heavy rain shifted the strongest hazard regions to the southern portion of the outflow. According to the simulation this second surge was associated with melting of graupel aloft and generated the overall strongest downdraft speeds and wind-shear. During this phase of development, the microburst was again encountered by NASA (Event #143), and in-situ and model data show a complex asymmetric F-factor field. The complex hazard field exists, even though the simulation shows a nearly symmetric *region* of outflow. The model data also indicates that regions of upflow and performance-increase (positive F-factor) are embedded within the microburst outflow, as was true in an earlier case-simulation of another Florida microburst[6]. Hence, hazard regions may be asymmetric and complex even in the weak ambient wind conditions typical of Florida's summer season. Following the time of peak outflow and wind-shear hazard, the outflow continues to expand becoming a macroburst, although with embedded microbursts. The model simulation, in-situ (Event #144), and TDWR data indicate that the embedded microbursts are of weaker magnitude than the primary microburst during intense phase (at least true for this case study).

Local correlation between F-factor and either temperature drop or temperature gradient is not apparent in the data from the simulation. However, as predicted by the empirical formula for maximum wind differential from temperature drop[5,9], the simulated temperature drop of about 6°C at the surface corresponds to the simulated peak wind change (at 70 m AGL) of 32 m/s. At flight level (roughly 325 m AGL) and at 37 min simulation time, the maximum temperature drop was 3.5° C, almost half the magnitude of the temperature drop at the ground. Hence as shown in the axisymmetric experiment of wet microburst, the magnitude of temperature drop is greatest near the ground and markedly decreases with altitude[4,5].

REFERENCES

1. Proctor, F. H., 1987: The Terminal Area Simulation System. Volume I: Theoretical formulation. NASA Contractor Rep. 4046, NASA, Washington, DC, 176 pp. [Available from NTIS]

2. Proctor, F. H., 1987: The Terminal Area Simulation System. Volume II: Verification Experiments. NASA Contractor Rep. 4047, NASA, Washington, DC, 112 pp. [Available from NTIS]

3. Proctor, F. H., 1988: Numerical simulation of the 2 August 1985 DFW microburst with the three-dimensional Terminal Area Simulation System. Preprints Joint Session of 15th Conf. on Severe Local Storms and Eighth Conf. on Numerical Weather Pred., Baltimore, Amer. Meteor. Soc., J99-J102.

4. Proctor, F. H., 1988: Numerical simulations of an isolated microburst. Part I: Dynamics and structure. J. Atmos. Sci., 45, 3137-3160.

5. Proctor, F. H., 1989: Numerical simulations of an isolated microburst. Part II: Sensitivity experiments. J. Atmos. Sci., 46, 2143-2165.

6. Proctor, F. H., 1990: Three-dimensional numerical simulation of a Florida microburst: The 7 July 1990 Orlando event. Airborne Wind Shear Detection and Warning Systems, Third Combined Manufacturers' and Technologists' Airborne Wind Shear Review Meeting, Hampton, VA, NASA Conf. Publication 10060, Part I, 81-103. [Available from NTIS]

7. Proctor, F. H., and R. L. Bowles, 1990: Three-dimensional simulation of the Denver 11 July storm of 1988: An intense microburst event. Preprints, 16th Conf. on Severe Local Storms and the Conf. on Atmos. Electricity, Kananaskis Park, Amer. Meteor. Soc., 373-378.

8. Proctor, F. H., and R. L. Bowles, 1992: Three-dimensional simulation of the Denver 11 July 1988 microburst-producing storm. Accepted for publication in Meteorol. and Atmos. Phys., 47.

9. Proctor, F. H., 1989: A relation between peak temperature drop and velocity differential in a microburst. Preprints Third International Conf. on the Aviation Wea. System., Anaheim, Amer. Meteor. Soc., 5-8.

TERMINAL AREA SIMULATION SYSTEM (TASS)

[ALSO KNOWN AS THE NASA WINDSHEAR MODEL]

- 3-D TIME DEPENDENT EQUATIONS FOR COMPRESSIBLE NONHYDROSTATIC FLUIDS

- PROGNOSTIC EQUATIONS FOR 11 VARIABLES
  1. 3-COMPONENTS OF VELOCITY
  2. PRESSURE
  3. POTENTIAL TEMPERATURE
  4. WATER VAPOR
  5. LIQUID CLOUD DROPLETS
  6. CLOUD ICE CRYSTALS
  7. RAIN
  8. SNOW
  9. HAIL/GRAUPEL

- 1st-ORDER SUBGRID TURBULENCE CLOSURE WITH RICHARDSON NUMBER DEPENDENCY

- SURFACE FRICTION LAYER BASED ON MONIN-OBUKHOV SIMILARITY THEORY

- OPEN LATERAL BOUNDARY CONDITIONS ALLOWING MINIMAL REFLECTION

- BULK PARAMETERIZATIONS OF CLOUD MICROPHYSICS

SLIDE 1

Table 1. Salient Characteristics of TASS 2.4

Compressible, nonhydrostatic equation set
Non-Boussinesq formulation for density variations
Three-dimensional staggered grid with stretched vertical spacing
Movable, storm-centering mesh
Explicit time-split, second-order, Adams-Bashforth time differencing and second-order quadratic-conservative space differencing for velocity and pressure
Fourth-order quadratic-conservative space differencing and third-order Adams-Bashforth time differencing for temperature and water-vapor equations
Third-order time/space differencing with upstream-biased quadratic interpolation for liquid and frozen water substance equations
Radiation boundary conditions applied to open lateral boundaries
Filter and Sponge applied to top four rows in order to diminish gravity wave reflection at top boundary
No explicit numerical filtering applied to interior points
Surface friction layer based on Monin-Obukhov Similarity theory
Smagorinsky subgrid-turbulence closure with Richardson number dependence
Liquid and ice-phase microphysics
Inverse-exponential size distributions assumed for rain, hail/graupel, and snow
Raindrop intercept function of amount of rainwater^5
Snow treated as spherical, low-density graupel-like snow particles
Wet and dry hail growth
Accumulated precipitation advected opposite of grid motion, so as to remain ground relative

Table 2. Cloud Microphysical Interactions

Accretion of cloud droplets by rain
Condensation of water vapor into cloud droplets
Berry-Reinhardt formulation for autoconversion of cloud droplet water into rain
Evaporation of rain and cloud droplets
Spontaneous freezing of supercooled cloud droplets and rain
Initiation of cloud ice crystals
Ice crystal and snow growth due to riming
Vapor deposition and sublimation of hail/graupel, snow, and cloud ice crystals
Accretion by hail/graupel of cloud droplets, cloud ice crystals, rain, and snow
Contact freezing of supercooled rain resulting from collisions with cloud ice crystals or snow
Production of hail/graupel from snow riming
Melting of cloud ice crystals, snow, and hail/graupel
Shedding of unfrozen water during hail wet growth
Shedding of water from melting hail/graupel and snow
Conversion of cloud ice crystals into snow
Accretion by snow of cloud droplets, cloud ice crystals, and rain
Evaporation or vapor condensation on melting hail/graupel and snow

Orlando, Fl, 20 June 1991, Simulation

INPUT DATA / ASSUMPTIONS

PHYSICAL DOMAIN SIZE

- O X,Y: 15 KM x 15 KM
- O Z: 18 KM

COMPUTATIONAL RESOLUTION

- O HORIZONTAL - 150 M (103 X 103 GRID POINTS)
- O VERTICAL - 70 M NEAR GROUND STRETCHING TO 440 M AT 18 KM (72 LEVELS)

CONVECTIVE INITIATION AT MODEL TIME ZERO

- O SPHEROIDAL THERMAL IMPULSE
- O DIMENSIONS - 7 KM HORIZONTAL x 1.25 KM VERTICAL
- O AMPLITUDE - 1.5^{O} C

SOUNDING OBSERVED NEAR TIME AND LOCATION OF STORM (from special rawinsonde launch 2035 UTC)

SUB-CLOUD HUMIDITY AND TEMPERATURE MODIFIED USING NASA AIRCRAFT MEASUREMENTS TAKEN NEAR THE TIME AND LOCATION OF THE STORM

SLIDE 2

Orlando, Fl, 20 June 1991
Special sounding - 2035 UTC

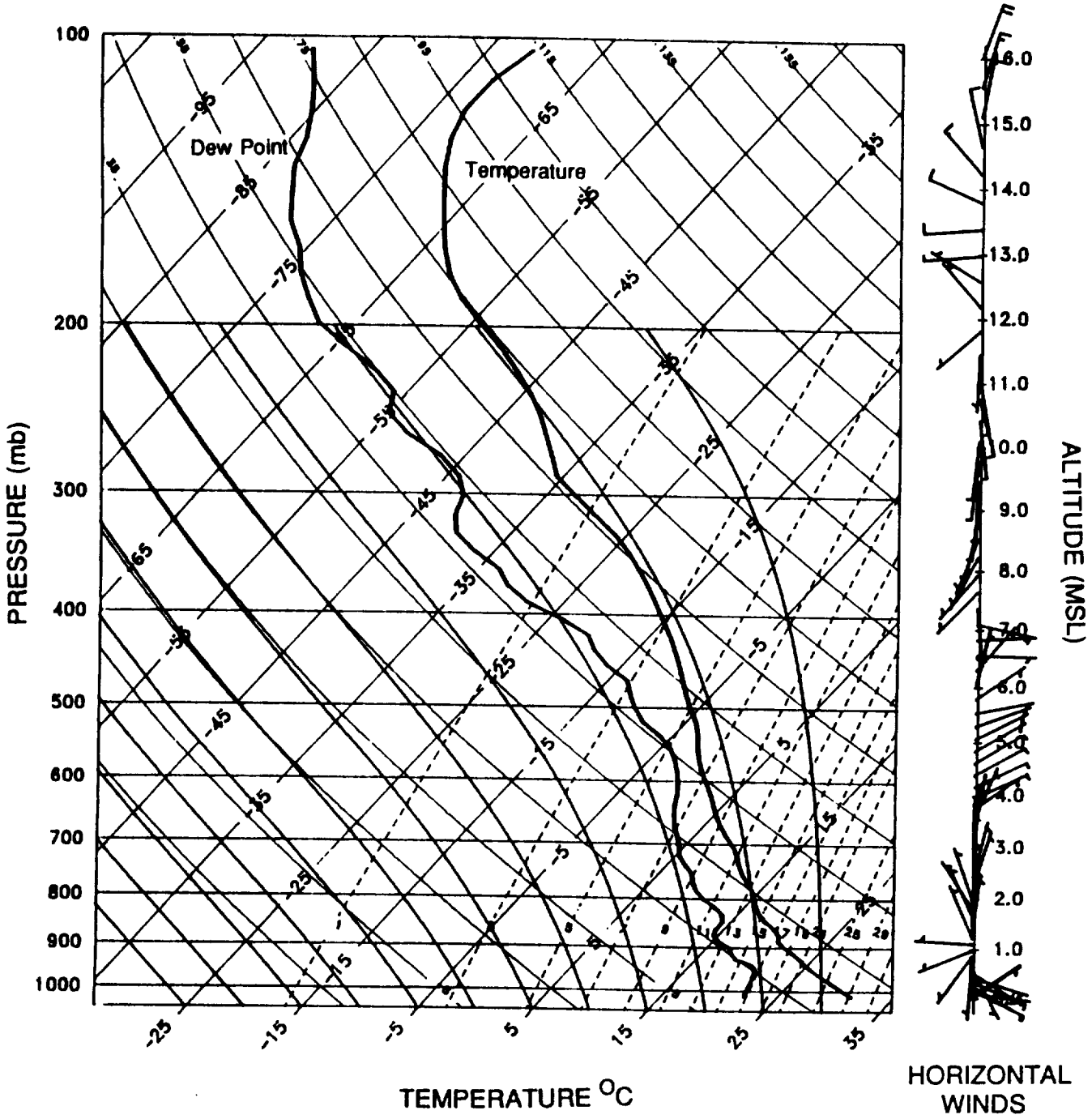

SLIDE 3

20 JUNE 1991 MICROBURST

- MICROBURST ENCOUNTERED BY NASA AIRCRAFT 3 TIMES
  1. FIRST ENCOUNTER (~2041 UTC) DURING INTENSIFICATION STAGE (EVENT #142).
  2. 2ND ENCOUNTER (~2046) DURING PEAK INTENSITY (EVENT #143).
  3. 3RD ENCOUNTER (~2051) DURING MACROBURST STAGE (EVENT #144).

- DURING INTENSIFICATION PHASE, MODEL AND OBSERVED RESULTS SHOW STRONGEST SHEAR AND DOWNFLOW IN NORTHERN REGION OF OUTFLOW.

- MODEL AND OBSERVED RESULTS INDICATE MAXIMUM SHEAR AND DOWNFLOW IN SOUTHERN REGION OF OUTFLOW DURING PEAK INTENSITY.

- MODEL RESULTS INDICATE MICROBURST INITIATED BY RAIN FORMED THROUGH COLLECTION-COALESCENCE.

- ACCORDING TO MODEL SIMULATION, THE MICROBURST IS ENHANCED DURING PEAK-INTENSITY PHASE BY A SECOND SURGE OF PRECIPITATION.

- THIS SECOND SURGE -- ASSOCIATED WITH RAIN FROM MELTING GRAUPEL -- GENERATES STRONGEST SHEAR AND DOWNDRAFT SPEEDS IN SOUTHERN SECTOR.

20 JUN 1991 ORLANDO MICROBURST

Velocity Differential Comparison at 190 M AGL

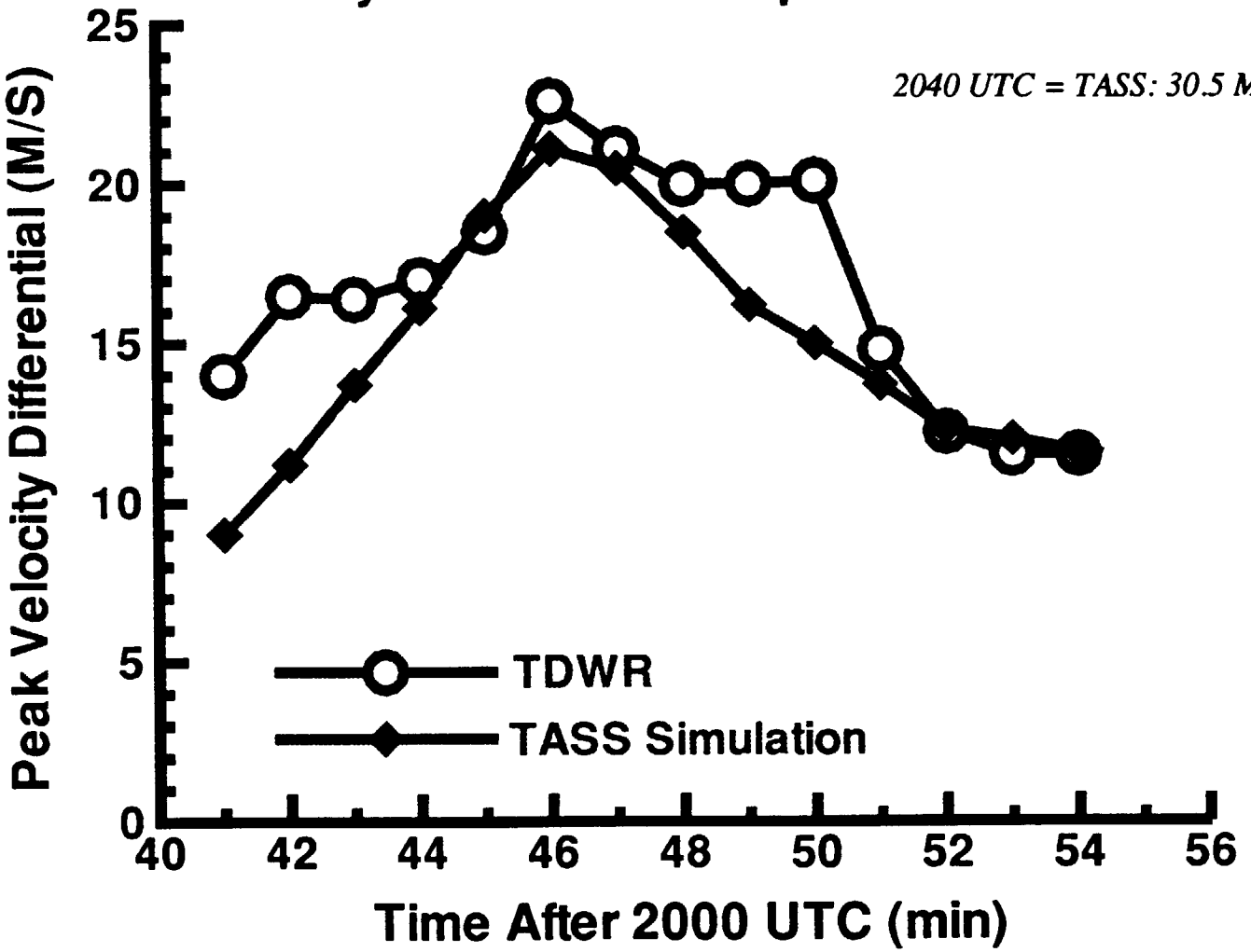

20 JUN 1991 ORLANDO MICROBURST

Peak 1-Km Avg F-Factor Comparison at 190 M AGL

(Assumes 110 m/s groundspeed)

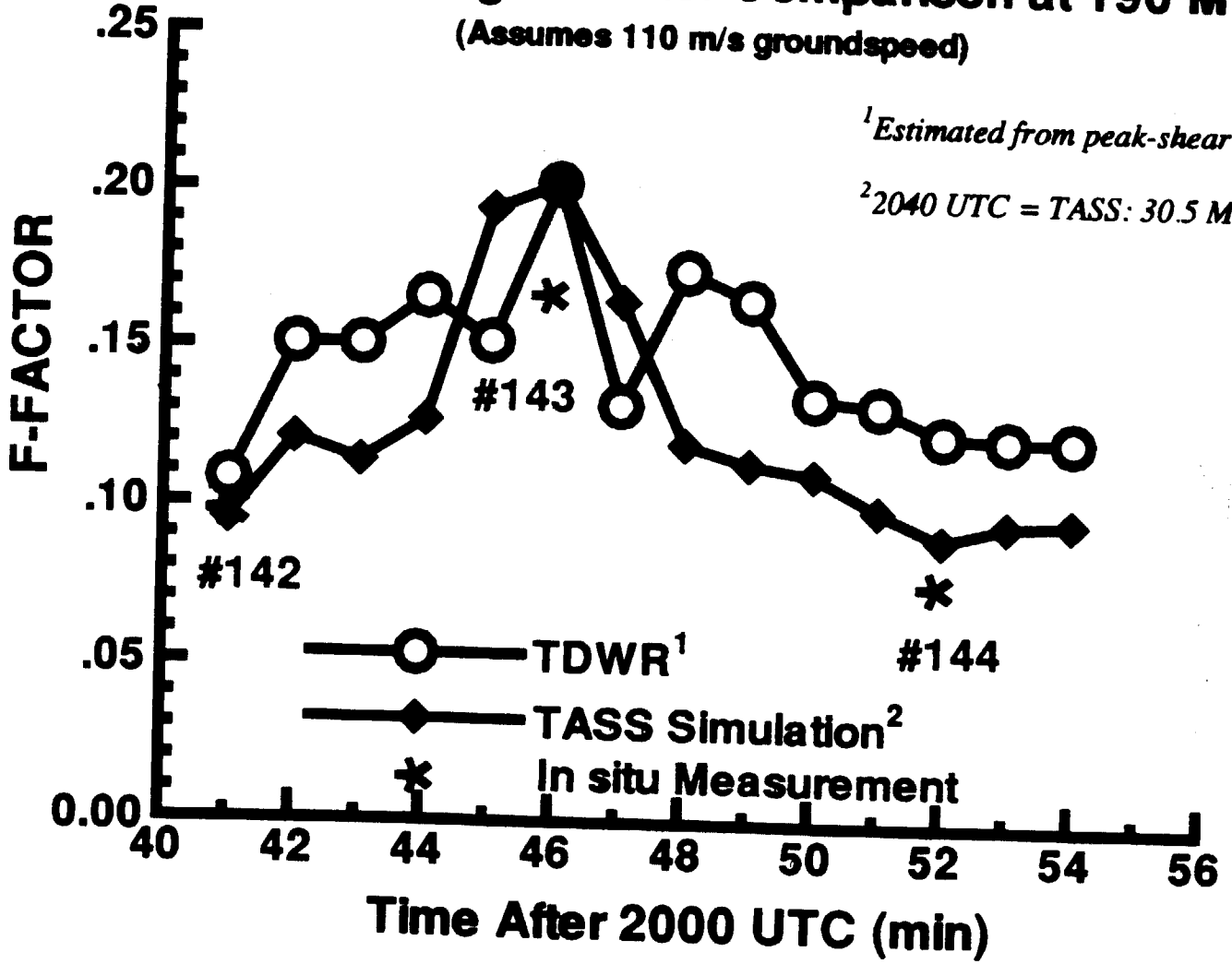

[1]Estimated from peak-shear segments

[2]2040 UTC = TASS: 30.5 Min

TASS 3-D SIMULATION -- ORLANDO MICROBURST
3-D PERSPECTIVE OF STORM

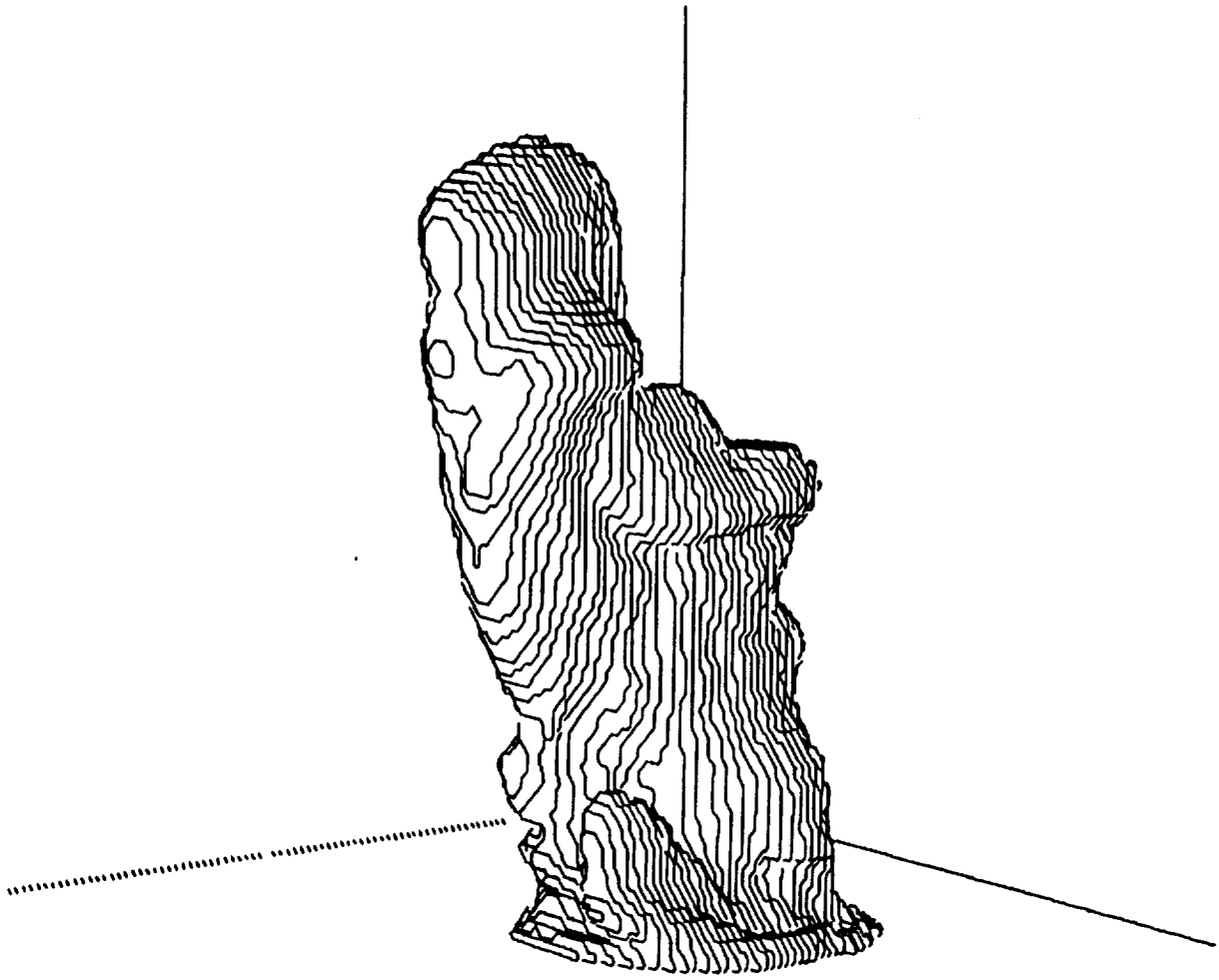

10 DBZ RADAR REFLECTIVITY SURFACE VIEWED FROM NE
AT 36 MIN (2045 UTC)
STORM TOP AT 14 KM

ORIGINAL PAGE
COLOR PHOTOGRAPH

ORLANDO 20 JUNE 1991 MICROBURST SIMULATION

VELOCITY ALONG TDWR RADIAL AT 190 M AGL

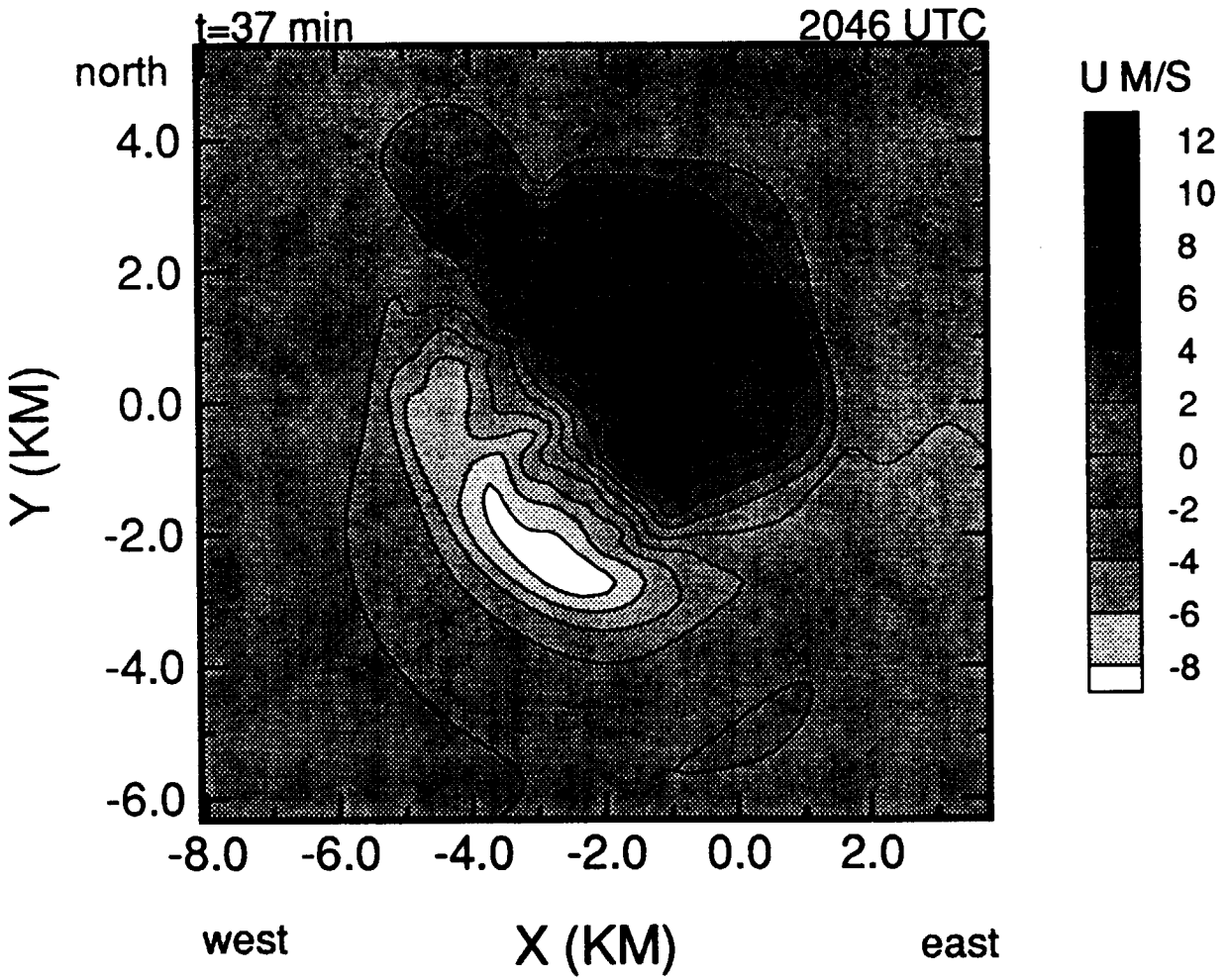

COLOR PHOTOGRAPH

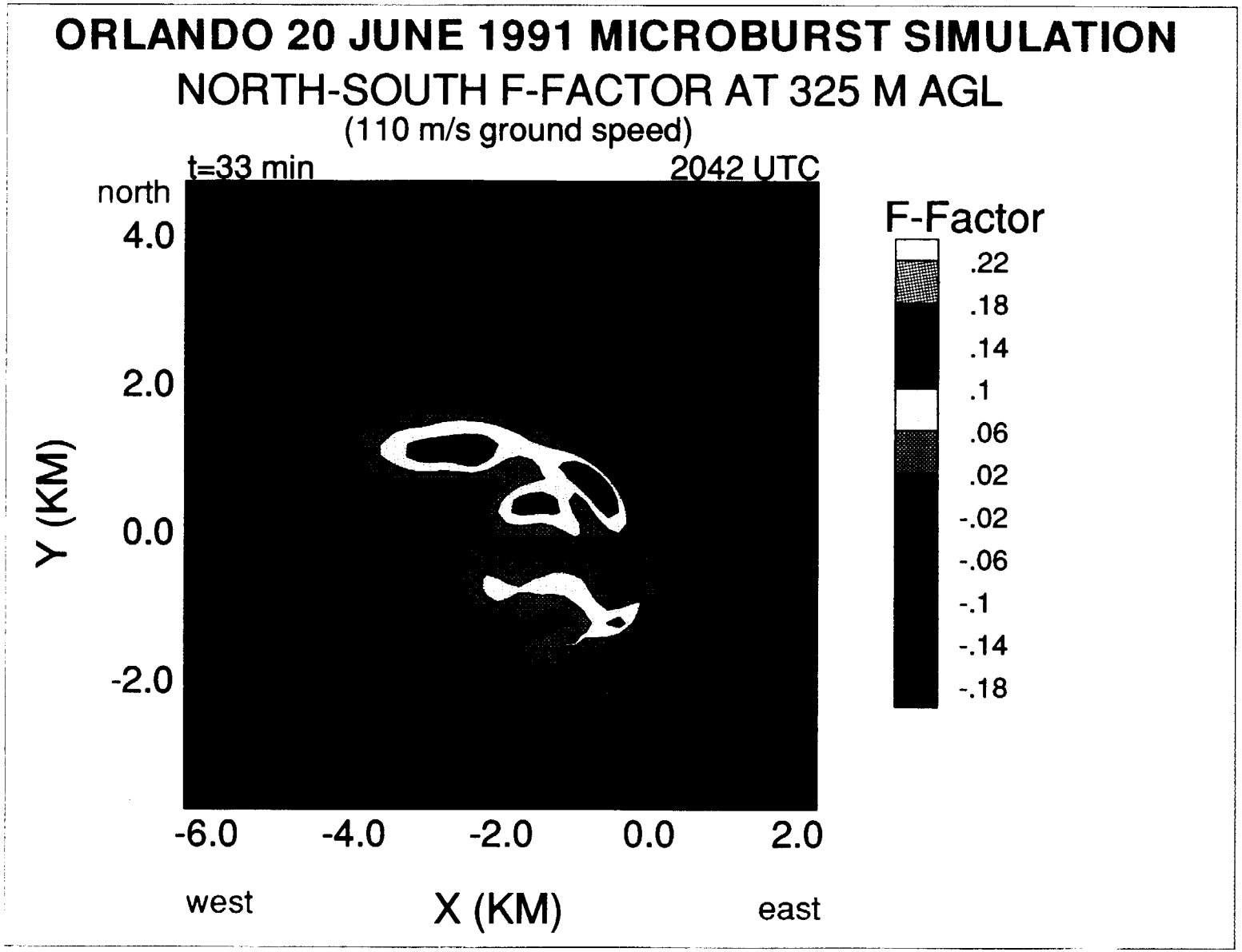

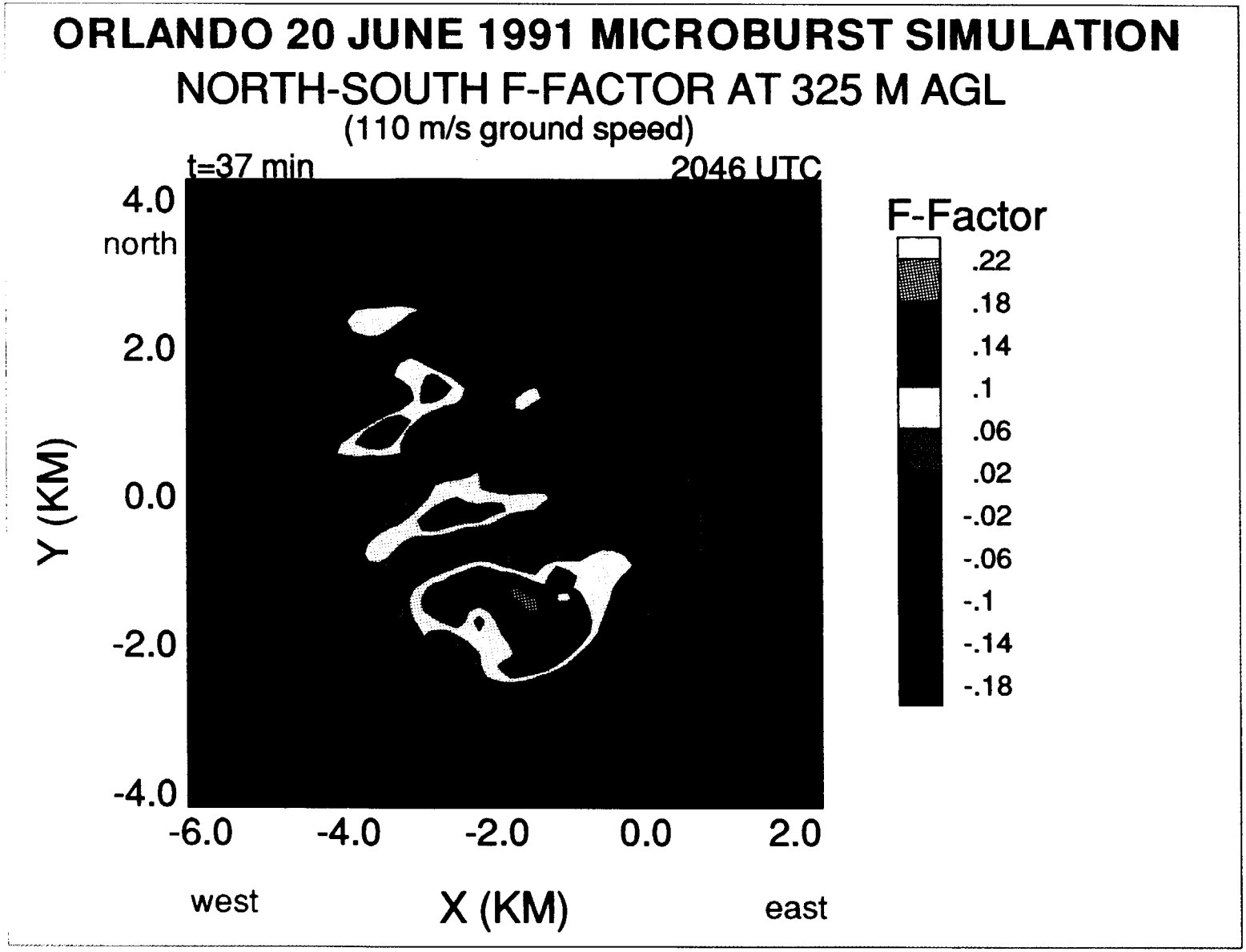
ORLANDO 20 JUNE 1991 MICROBURST SIMULATION
NORTH-SOUTH F-FACTOR AT 325 M AGL
(110 m/s ground speed)
t=37 min
2046 UTC
4.0
north
2.0
0.0
-2.0
-4.0
Y (KM)
-6.0
-4.0
-2.0
0.0
2.0
west
X (KM)
east
F-Factor
.22
.18
.14
.1
.06
.02
-.02
-.06
-.1
-.14
-.18

ORIGINAL PAGE
COLOR PHOTOGRAPH

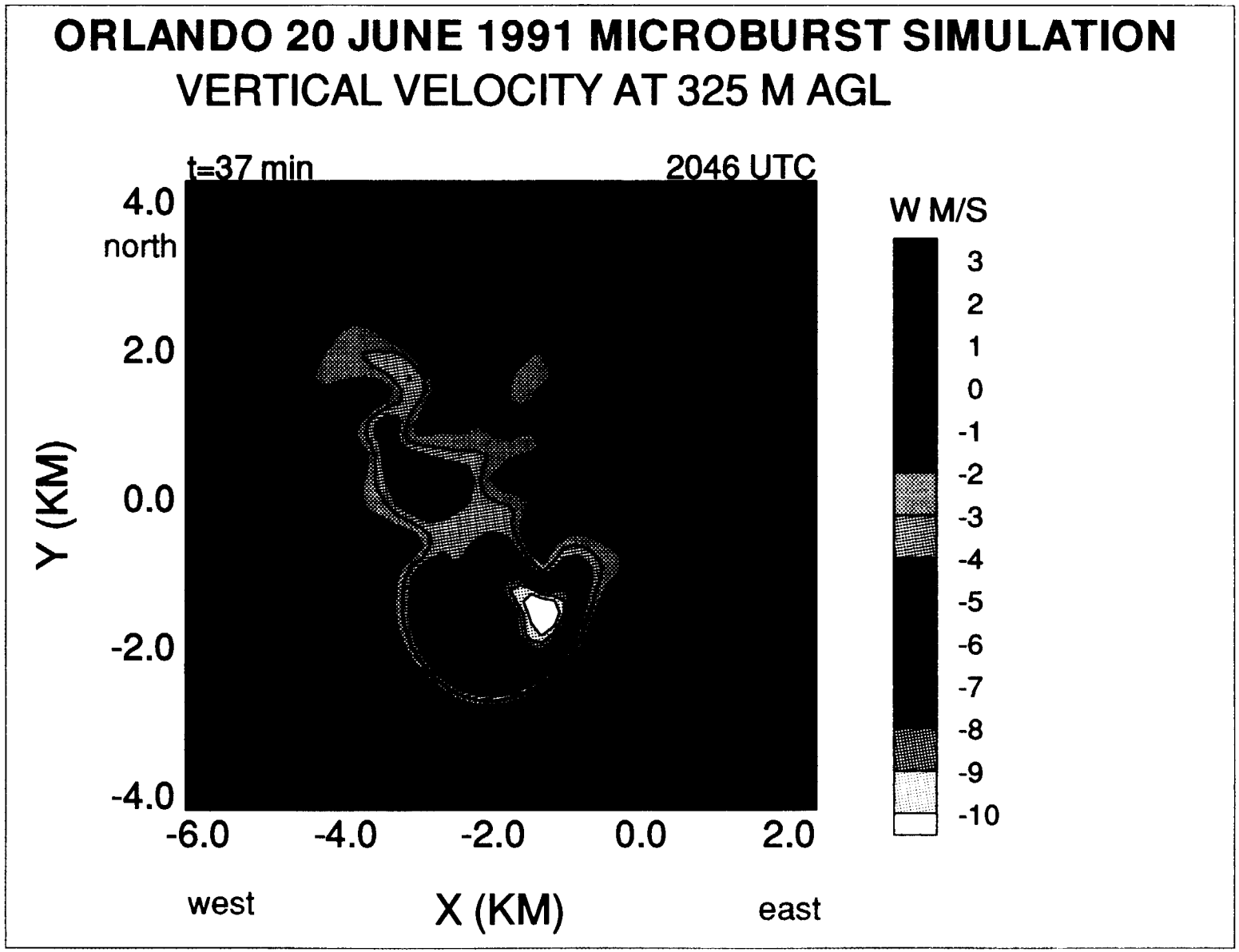
ORLANDO 20 JUNE 1991 MICROBURST SIMULATION
VERTICAL VELOCITY AT 325 M AGL
t=37 min
2046 UTC
W M/S
3
2
1
0
-1
-2
-3
-4
-5
-6
-7
-8
-9
-10
4.0
north
2.0
0.0
-2.0
-4.0
Y (KM)
-6.0
-4.0
-2.0
0.0
2.0
west
X (KM)
east

ORIGINAL PAGE
COLOR PHOTOGRAPH

ORLANDO 20 JUNE 1991 MICROBURST SIMULATION

RADAR REFLECTIVITY AT 150 M AGL

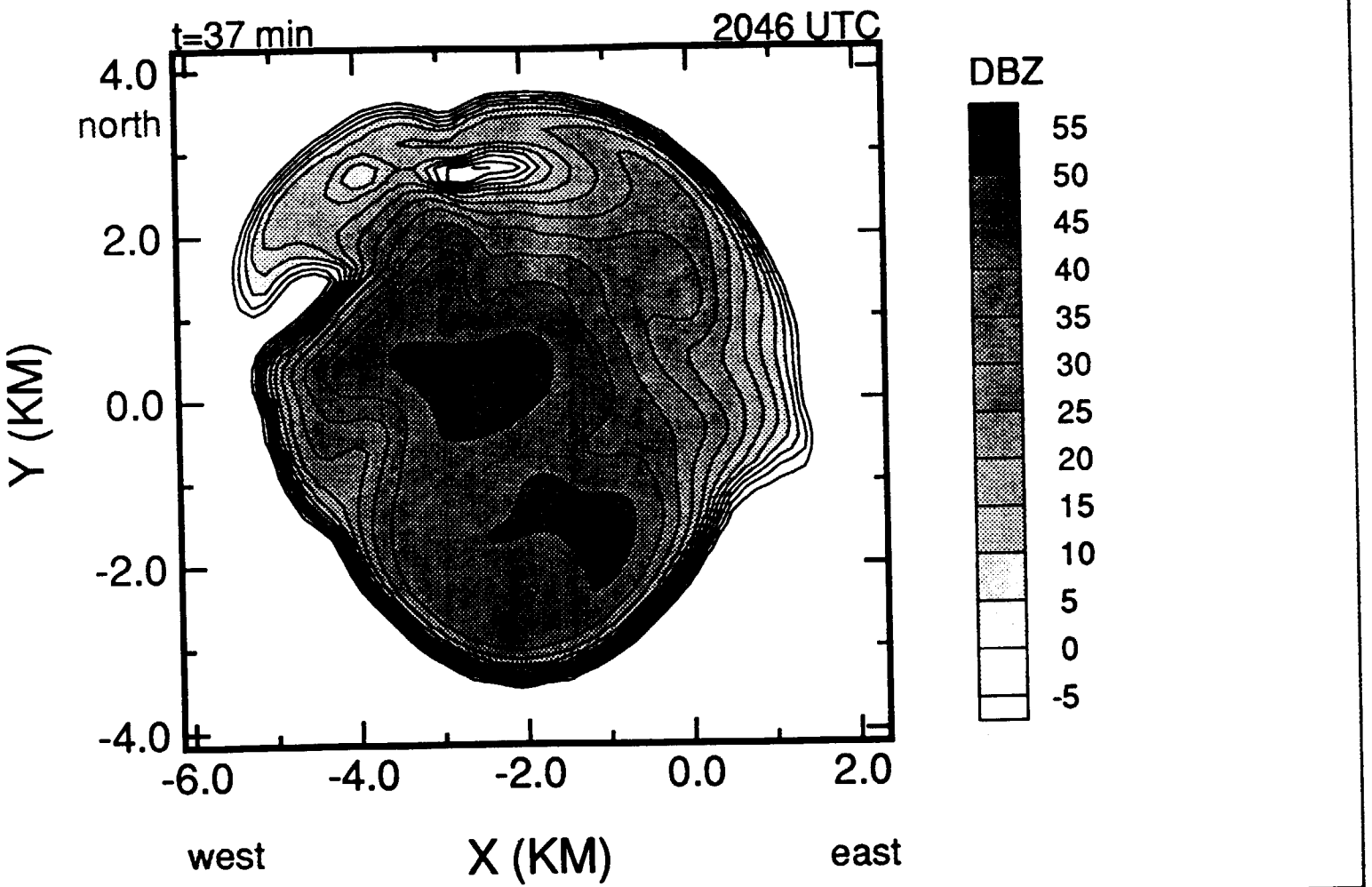

ORIGINAL PAGE
COLOR PHOTOGRAPH

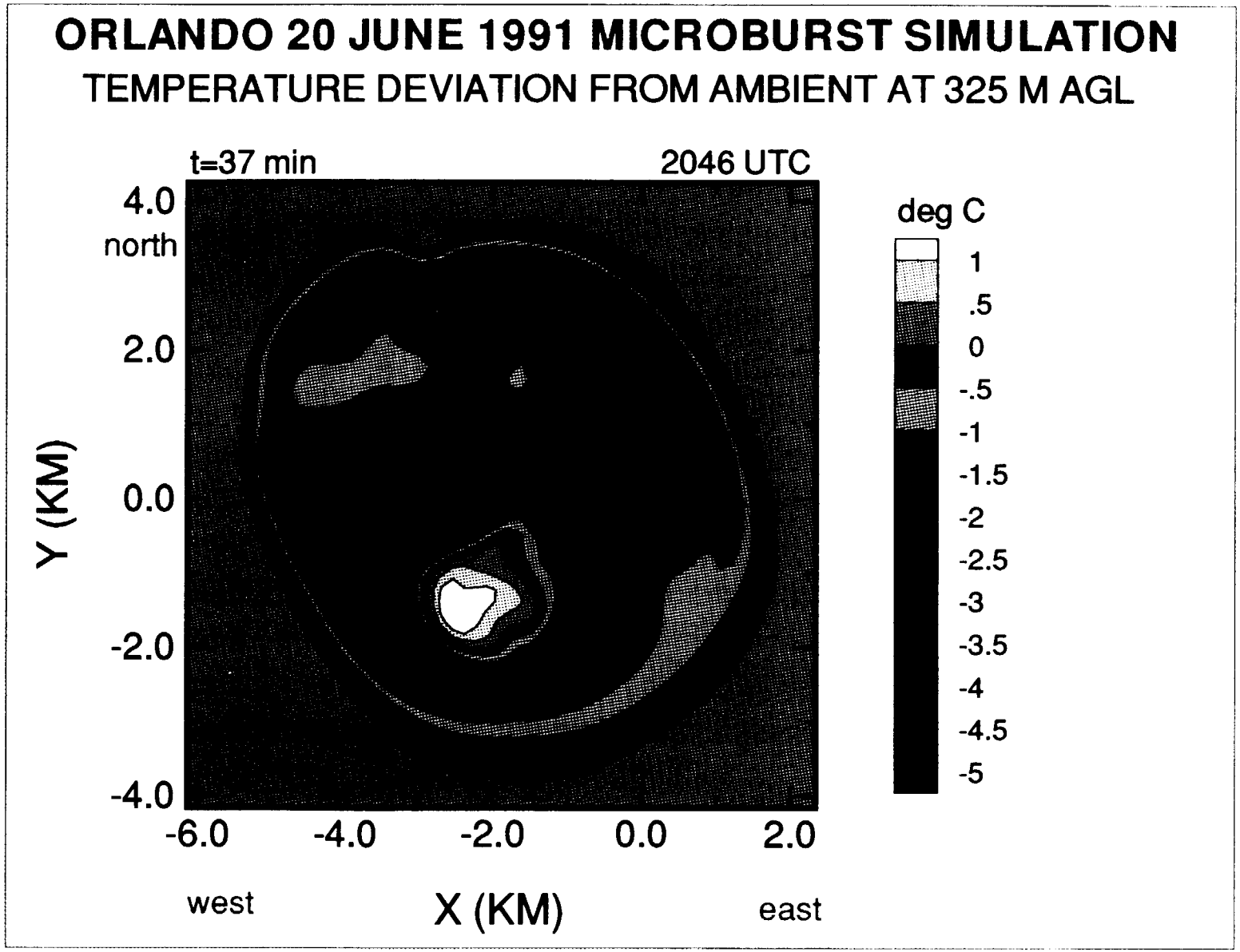

COLOR PHOTOGRAPH

ORLANDO 20 JUNE 1991 MICROBURST SIMULATION
N-S TEMPERATURE GRADIENT AT 325 M AGL

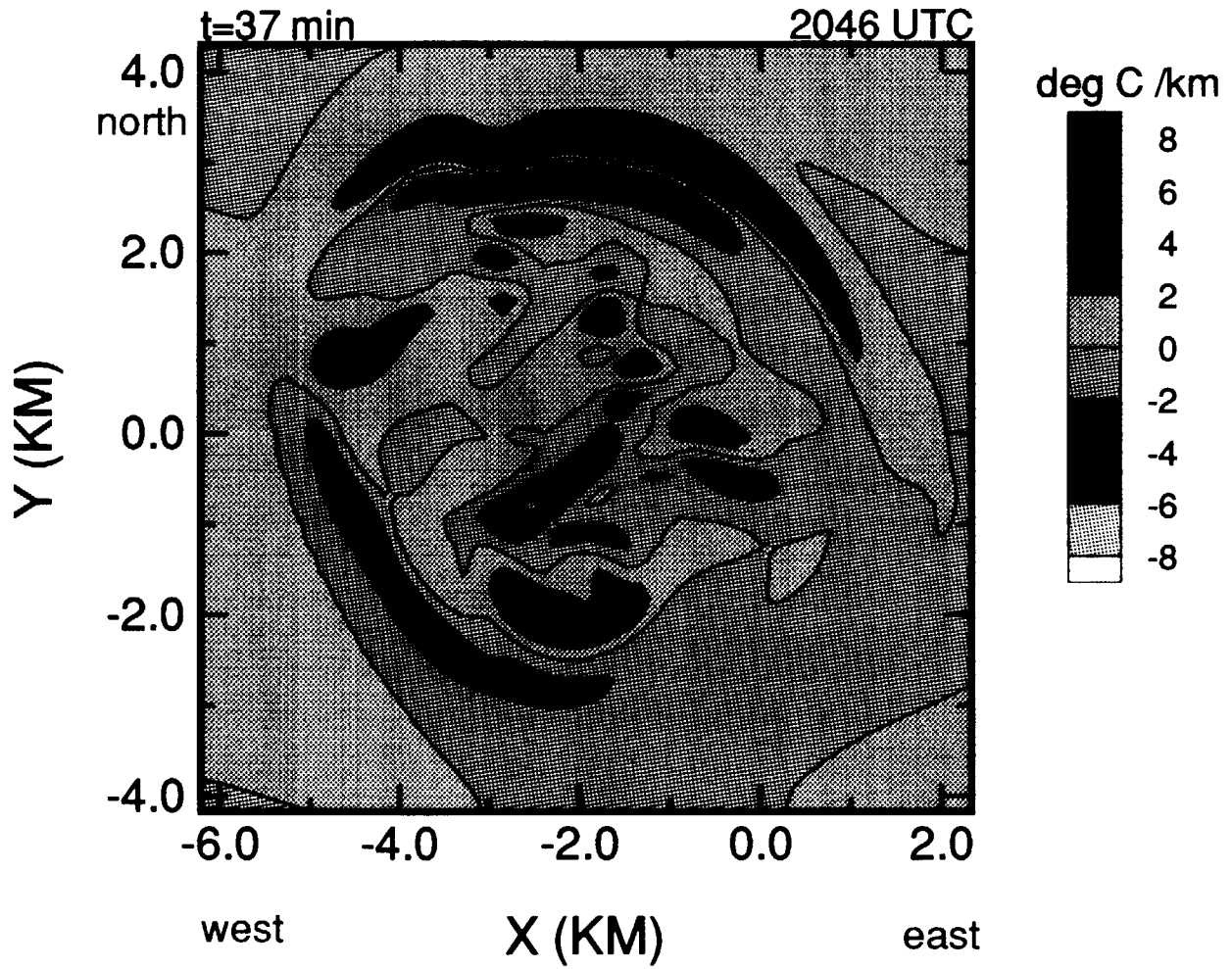

ORIGINAL PAGE
COLOR PHOTOGRAPH

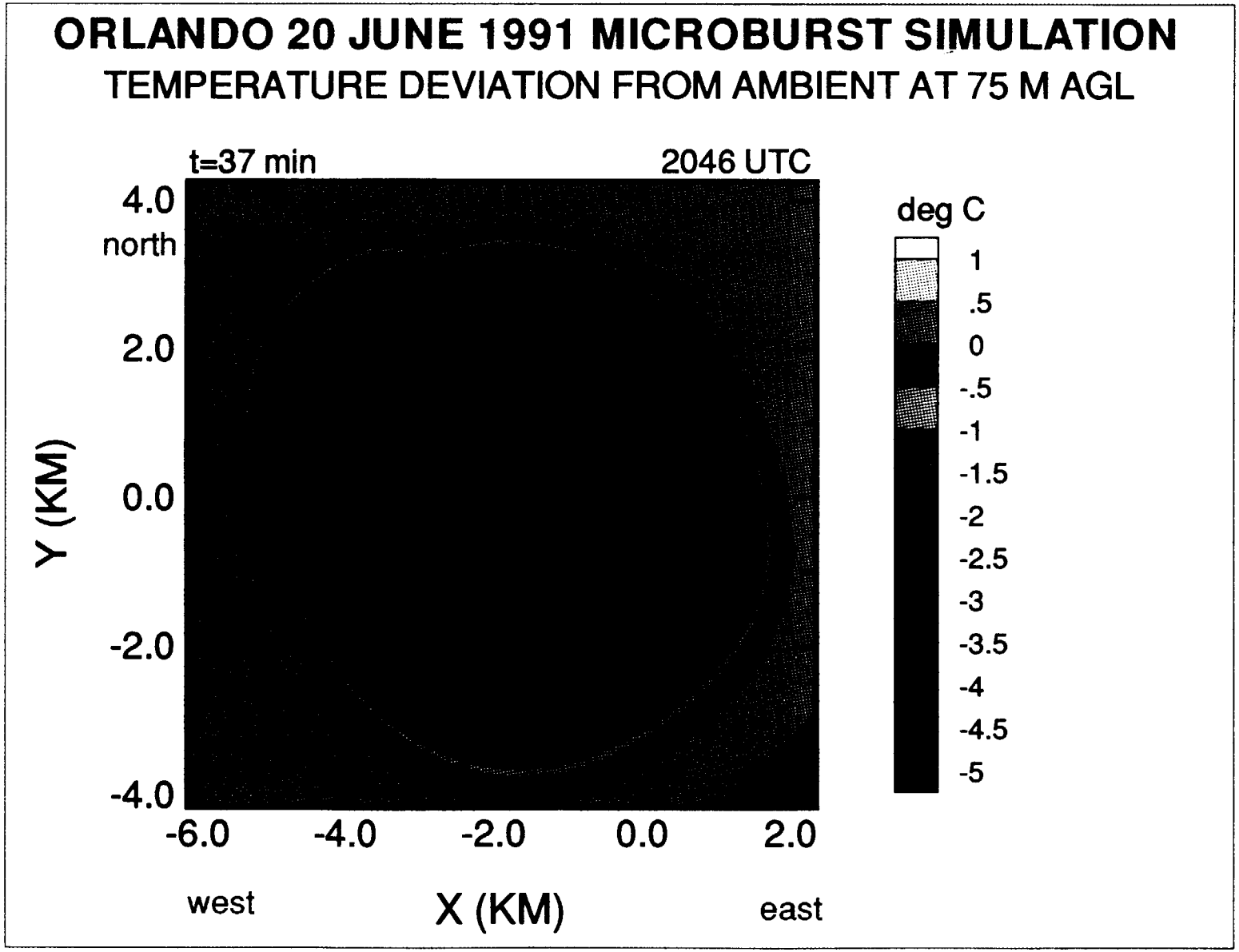

ORLANDO 20 JUNE MICROBURST SIMULATION

1-KM AVG. F-FACTOR AT 2046 UTC MODEL TIME

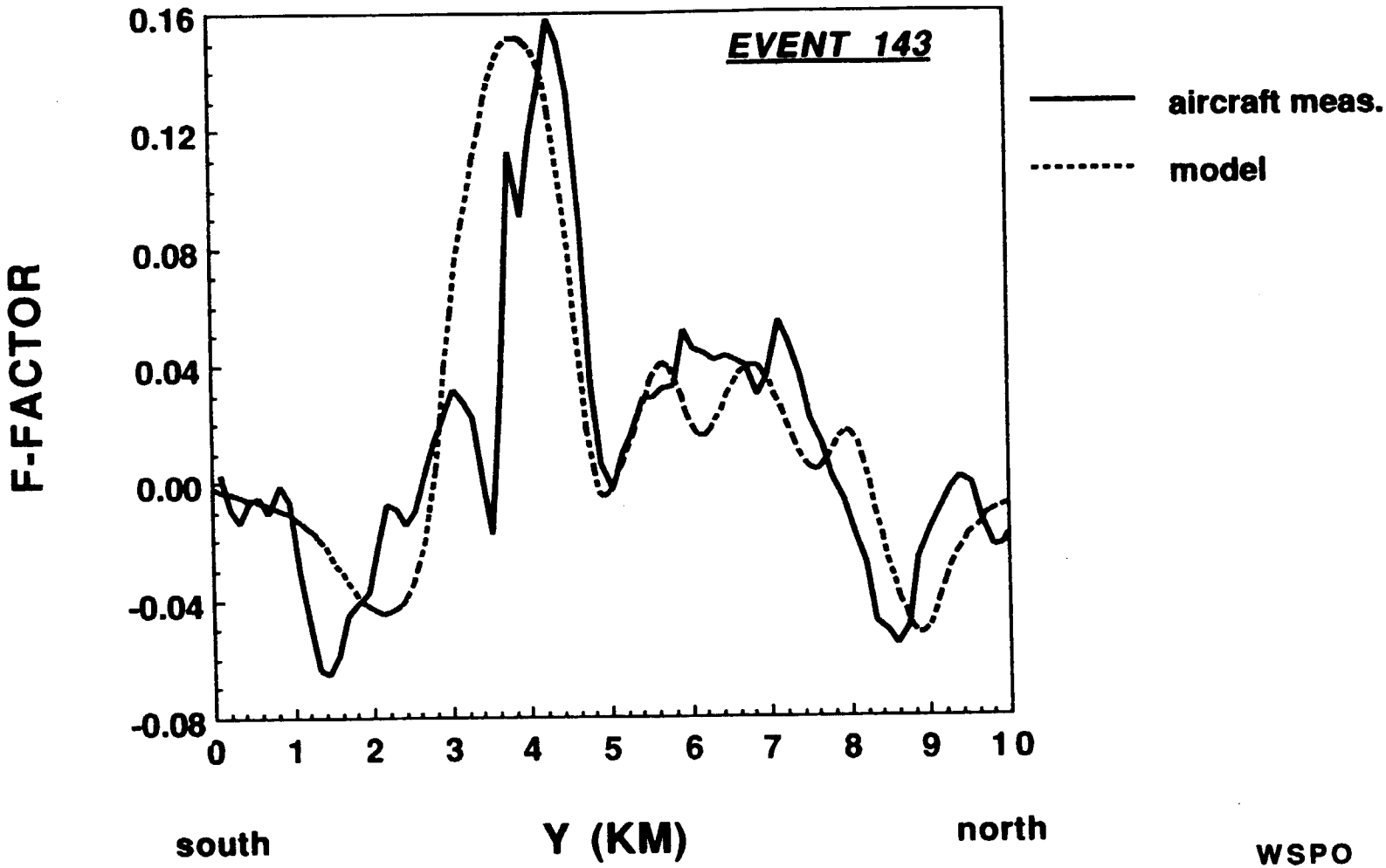

WSPO

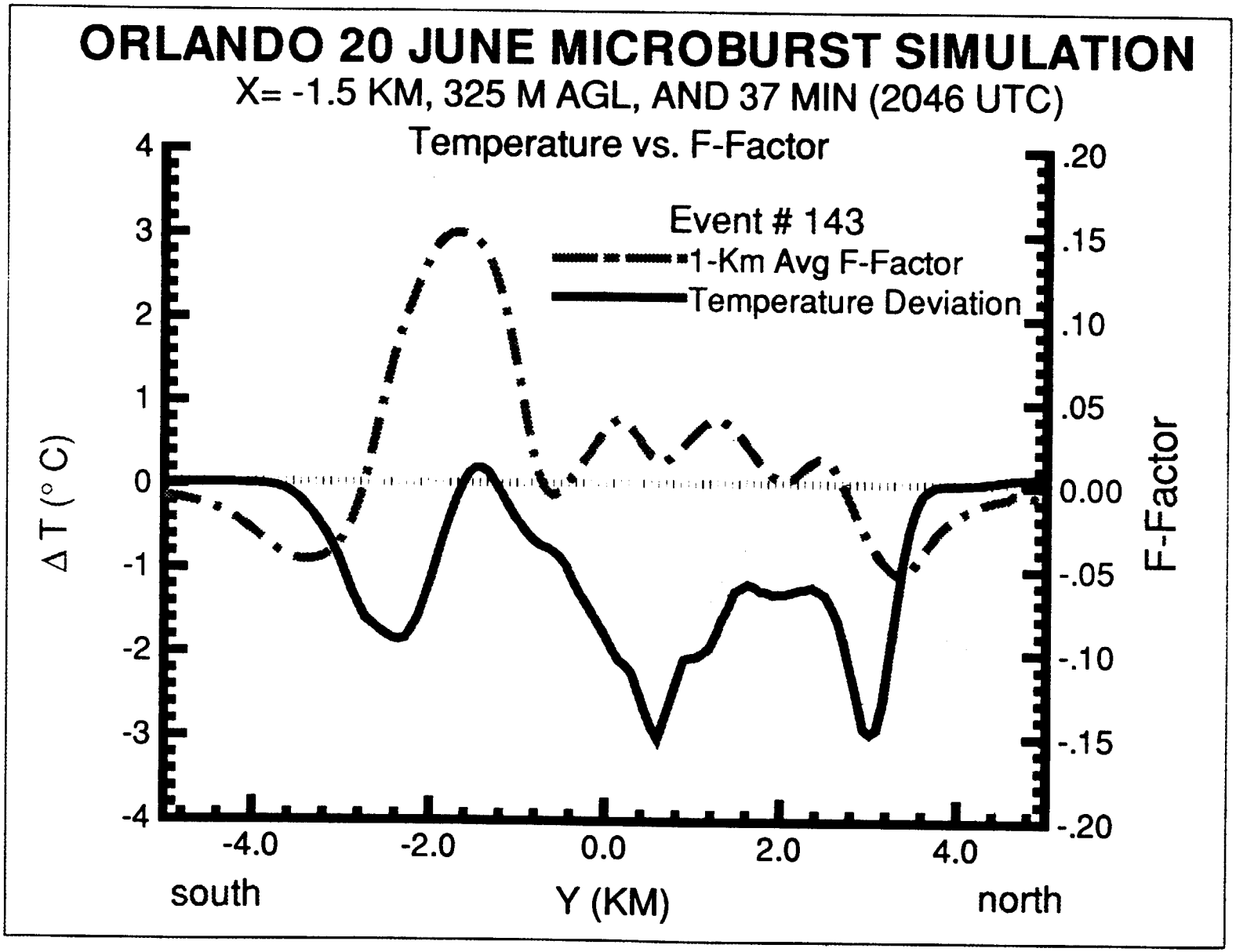
ORLANDO 20 JUNE MICROBURST SIMULATION
X= -1.5 KM, 325 M AGL, AND 37 MIN (2046 UTC)
Temperature vs. F-Factor
Event # 143
1-Km Avg F-Factor
Temperature Deviation
ΔT (°C)
F-Factor
4
3
2
1
0
-1
-2
-3
-4
.20
.15
.10
.05
0.00
-.05
-.10
-.15
-.20
-4.0
-2.0
0.0
2.0
4.0
south
Y (KM)
north

ORLANDO 20 JUNE 1991 MICROBURST SIMULATION

Wind Vectors

South-North Vertical Cross Section at 37 min (2046 UTC)

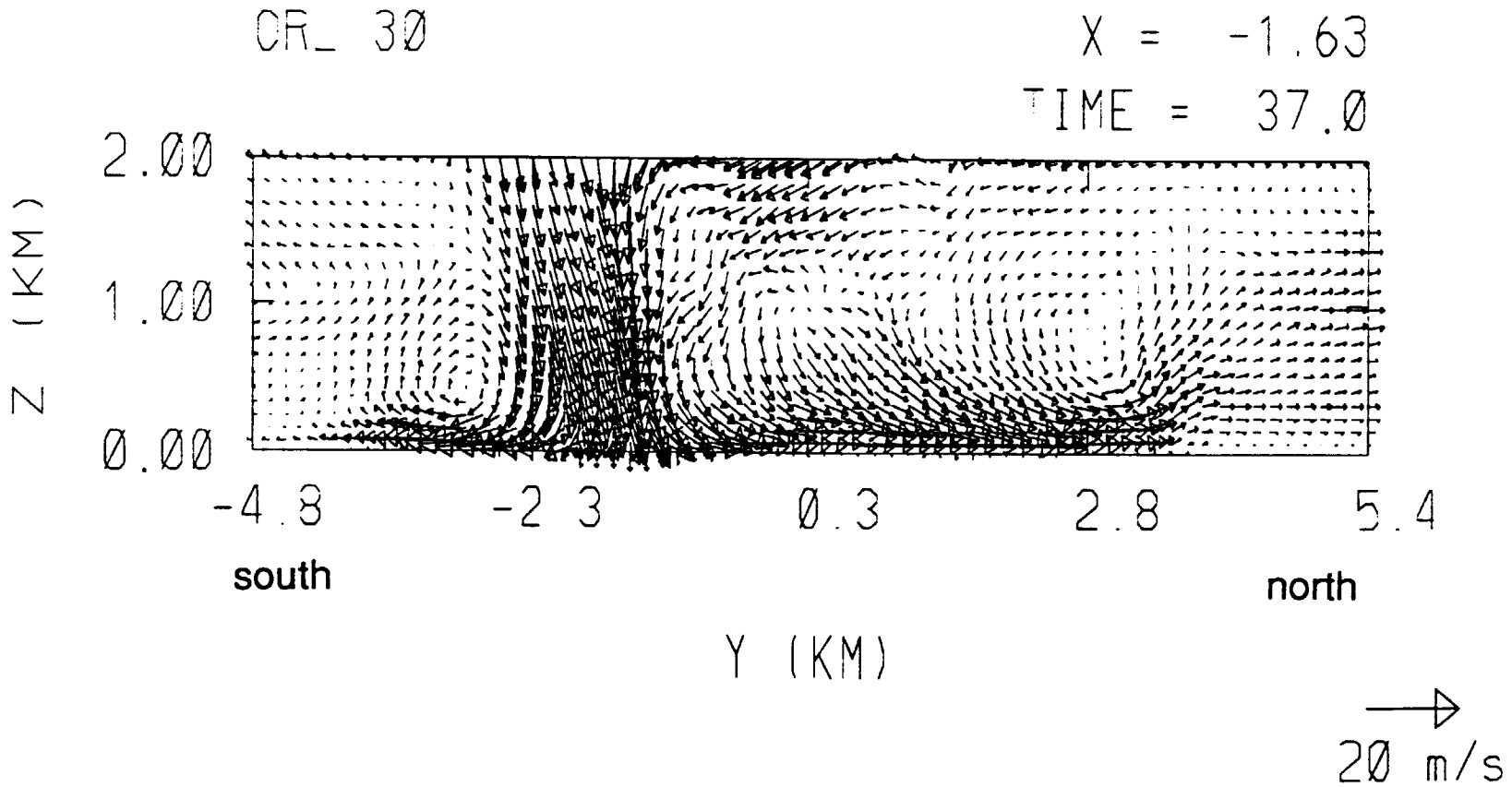

SUMMARY OF ORLANDO SIMULATION

- WET MICROBURST WITH HAZARDOUS WIND SHEAR

- GOOD AGREEMENT BETWEEN SIMULATION AND OBSERVATION OF EVENT

- COMPLEX MICROBURST STRUCTURE:
  1. MULTIPLE DOWNDRAFT SURGES
  2. MULTIPLE DIVERGENCE CENTERS EMBEDDED WITHIN OUTFLOW
  3. AREAS OF UPWARD MOTION EMBEDDED WITHIN OUTFLOW
  4. NONCLASSIC OUTFLOW AND F-FACTOR PROFILES

- MODELED ΔV FUNCTION OF ALTITUDE AND DIRECTION OF SEGMENT: PEAK ΔV OF 32.0 M/S ALONG EAST-WEST SEGMENT AT 70 M AGL .VS. 21.1 M/S ALONG SIMULATED TDWR RADIAL (NNE - SSW SEGMENT AT 190 M AGL)

- PEAK TEMPERATURE DROP OF ~6^{0} C OCCURS AT TIME OF MICROBURST PEAK INTENSITY

- SIMULATED RAINFALL RATES EXCEED 5 IN/HR AND 1-Km AVERAGED F-FACTORS EXCEED .15

- REGION OF PEAK WIND-SHEAR HAZARD DOES NOT CORRELATE LOCALLY WITH PEAK TEMPERATURE DROP

Three-Dimensional Numerical Simulation of the 20 June 1991, Orlando Microburst
Questions and Answers

Q: Not recorded

A: Fred Proctor (NASA Langley) - All my fields are assumed to be horizontally homogenous, in other words, they are constant horizontally but they vary in the vertical. There have been a lot of studies that have shown that storms are really determined by the vertical structure of the atmosphere. That is really what is playing a larger role in creating all these complex fields. The winds change direction with height as well as the temperature and humidity and so forth. Exactly how it's doing that I can't answer.

Q: (Unknown) - Have you correlated the DT measurements you have with the downdraft component of the F-factor as opposed to the total?

A: Fred Proctor (NASA Langley) - I haven't looked at that; I can't tell you.

Q: Kim Elmore (NCAR) - Did the downdraft initiate at the minimum QE level, since it was an area of a lot of coalescence? I was curious as to how deep it was?

A: Fred Proctor (NASA Langley) - I haven't looked at that yet, but usually in storms of this type I find them to form really close to the freezing level, wherever that may be.

Q: Kim Elmore (NCAR) - But it is still the evaporation of rain drops that is the primary driving force?

A: Fred Proctor (NASA Langley) - In this case yes.

Q: Kim Elmore (NCAR) - Is that common for the southeastern storms?

A: Fred Proctor (NASA Langley) - I would say it is probably a primary effect in most of the storms, but certainly not in all of them. You could get one in an atmosphere that was somewhat stable, relative to these. If you had relatively heavy rain fall rates, then you could probably drive them by mass loading.

Q: Kim Elmore (NCAR) - I was going to ask you how much of a role precipitation loading played?

A: Fred Proctor (NASA Langley) - I did not do that analysis for this storm, but I did for the one I presented at the last conference and the mass loading was a pretty small percentage of the total. Even though, in that storm, we had rainfall rates of 9 or 10 inches an hour. That was the Orlando 1990 Storm.